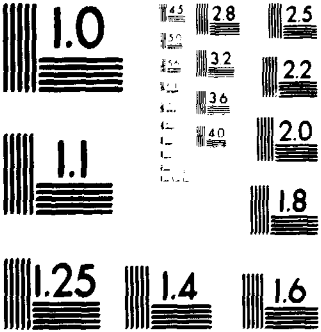

MICROCOPY RESOLUTION TEST CHART
NATIONAL BUREAU OF STANDARDS
STANDARD REFERENCE MATERIAL 1010a
(ANSI and ISO TEST CHART No. 2)

ISSN/0393-6333

RT/TIB/87/28

R. BARBINI, F. CIOCCI, G. DATOLI, A. TORRE, L. GIANNESSI

SPECTRAL PROPERTIES OF UNDULATORS RADIATION: A NUMERICAL METHOD

COMITATO NAZIONALE PER LA RICERCA E PER LO SVILUPPO DELL'ENERGIA NUCLEARE E DELLE ENERGIE ALTERNATIVE

ISSN / 0393-6333

COMITATO NAZIONALE PER LA RICERCA E PER LO SVILUPPO
DELL'ENERGIA NUCLEARE E DELLE ENERGIE ALTERNATIVE

SPECTRAL PROPERTIES OF UNDULATORS RADIATION: A NUMERICAL METHOD

Presented at the Undulator Magnets for Synchroton Radiation and Free *Electron Lasers Conference* (Trieste, 23-26 June 1987)

R. BARBINI, F. CIOCCI, G. DATTOLI, A. TORRE
ENEA - Dipartimento Tecnologie Intersettoriali di Base, Centro ricerche energia Frascati

L. GIANNESSI
ENEA - Guest

RT/TIB/87/28

Testo pervenuto nel settembre 1987

Progetto Enea: Progetto tecnologie ottiche ed elettro-ottiche (QU)

This report has been prepared by: Servizio Studi e Documentazione - ENEA, Centro Ricerche Energia Frascati, C.P. 65 - 00044 Frascati, Rome, Italy.
This Office will be glad to send further copies of this report on request.

Summary - We present the results of a numerical code dedicated to the analysis of the spectral features of the undulator radiation.

The developed numerical model includes the near-field effects, the inhomogeneous broadening due to the electron beam energy spread and emittances and the magnetic field random magnetization errors.

Riassunto - Vengono presentati i risultati di un codice numerico dedicato all'analisi delle caratteristiche spettrali della radiazione emessa in ondulatore.

Tale codice numerico tiene conto degli effetti di **near-field**, degli allargamenti inomogenei dovuti allo spread di energia e alla emittanza radiale e verticale del fascio di elettroni ed inoltre delle disomogeneità del campo magnetico dell'ondulatore dovute ad errori casuali di magnetizzazione.

1 - INTRODUCTION

The radiation emitted by relativistic electrons moving in magnetic undulators is playing an increasingly central role both in pure and applied science. The undulators are indeed exploited as sources of synchrotron radiation more intense than that produced by conventional bending magnets(1), or as pump-fields of Free Electron Lasers (FEL)(2).

So a wide range of applications strongly demands reliable predictions on the detailed characteristics of the emission spectra, including the large number of parameters as e.g. the e-beam qualities and the magnetic field random errors.

The properties of the undulator radiation spectra have been thoroughly investigated; analytical(3) and numerical(4) models have been developed.

The analytical methods have been able to clarify the main features of the spectra as e.g. the harmonics structure and the angular behaviour.

These models suffer however of a number of drawbacks as the impossibility of including the detailed electron beam structure or the undulator real electron trajectory for measured magnetic field or the effects due to random magnetization errors. Also the modification induced by near-field effects can be studied with the analytical method with some difficulties(5) but they are naturally included within the framework of a numerical analysis(6).

In this note we will present the main results from a numerical code specifically aimed to analyze the undulator spectra in conditions not amenable for an analytical treatment. We will also present the prediction of the code for a specific experimental configuration.

2 - NUMERICAL RESULTS

The code we have utilized to understand the details of the undulator radiation spectra[6] is an extended version of the S-Luce code originally developed in ref.[4].

From the conceptual point of view this code does not present any particular difficulty, being grounded essentially on a direct integration of the Lienard-Wiechert potentials, i.e.[7]

$$\frac{d^2 I}{d\omega\, d\Omega} = \frac{e^2}{4\pi^2 c} \left| \int dt' \exp[i\omega(t' + |\underline{R}(t')|/c)] \frac{\underline{n}\times[(\underline{n}-\underline{\beta})\times\dot{\underline{\beta}}]}{(1-\underline{n}\cdot\underline{\beta})^2} \right|^2 \qquad (1)$$

The physical meaning of the various terms appearing in (1) is clarified by fig. 1 (For the other symbols see also tab. 1).

The structure of the code is synthetically displayed by the block scheme of fig. 2. We will not enter in more detailed discussion of the code which can be found in ref.[6].

In the following we will present the results relevant to

(a) Homogeneous broadening case and a comparison with the analytical results.

(b) Inhomogeneous case for different e-beam energy spread and emittances.

(c) Near field effects for both homogeneous and inhomogeneous cases.

(d) Electron trajectory for measured undulator field.

3 - SPECTRAL BRIGHTNESS HOMOGENEOUS CASE

In figs. 3.a,b,c we show three-dimensional pictures of the spectral brightness for both helical and linear undulators at K=1. Fig. 3.a is relevant to the helical undulator and it is also displayed the well known result that in this case the fundamental

Table 1. List of symbols used throughout this paper

Physical constants

e	electron charge
m_0	rest electron mass
c	light velocity

Undulator Parameters

L	undulator length
λ_u	undulator period
$N = L/\lambda_u$	number of periods
$\langle B^2 \rangle^{1/2}$	r.m.s. magnetic field
$K = e\langle B^2 \rangle^{1/2} \lambda_u / (2\pi m_0 c^2)$	undulator parameter
$h_{x,y}$	transverse magnetic field sextupolar terms

Beam parameters

β	electron velocity in c unit
$\gamma = E/(m_0 c^2)$	relativistic factor
σ_e	r.m.s. relative energy spread
$E_{x,y}$	r.m.s. emittances
$\mu_{x,y,e}$	normalized inhomogeneous bandwidth

Radiation parameters

$\omega_u = 2\pi c/\lambda_u$	resonant frequency
$r = \omega/(2\gamma^2\omega_u)$	dimensionless frequency

harmonic only is present on axis. In figs. 3.b,c is shown the linear undulator brightness, unlike the helical case odd harmonics are radiated on axis and it is also shown the spectrum dependence on the azimuth φ.

An idea of the angular dependence of the spectra is given in figs. 4 where the peak of the first three harmonics from a linear undulator with K=0.5 is plotted vs. $\gamma\vartheta$. The dotted line is relevant to the result obtained from an analytical approach and the discrepancy between the two predictions is remarkable. We must however underline that such disagreement tends to disappear with increasing K and with increasing value of the azimuth, while for the helical case the agreement is always very good.

4 - INHOMOGENEOUS BROADENING EFFECTS

The results of the previous section are relevant to an ideal beam with zero energy spread and emittances.

It is well known that both the energy spread and the emittances produce an inhomogeneous broadening of the spectrum linewidth and a reduction of the peak values. It has been shown in ref.[2] that the importance of the inhomogeneous contributions may be qualitatively inferred by the so called μ-parameters which are the ratio between the inhomogeneous width due to the beam qualitics and the homogeneous one.

Such parameters are listed below

$$\mu_{x,y} = 2\ N \sqrt{2|h_{x,y}|}\ \frac{K}{1+K^2}\ \frac{\gamma E_{x,y}}{\lambda_u}$$

$$\mu_{\varepsilon} = 4\ N\ \sigma_{\varepsilon} \qquad (2)$$

where $E_{x,y}$ are the emittances and σ_{ε} is the r.m.s. energy spread (for the remaining symbols see tab. 1). When $\mu < 1$ the effect of the inhomogeneous broadening is not particularly significant while it becomes dominant at $\mu > 1$. In fig. 5 the on axis spectral brightness of a linear undulator is shown for both homogeneous (dotted line) and inhomogeneous case with the parameters specified in the caption; it is evident a strong suppression and a shape distorsion of the higher harmonics and what is remarkable is the presence of an even harmonic which is absolutely forbidden on axis in the homogeneous case. The catastrophic effect of the inhomogeneous broadening is shown in fig. 6 where all the μ are taken to be of the order of unity.

Finally in fig. 7 we show the effect of the inhomogeneous broadening on the axis of a 20 period helical undulator. The picture is self-explaining and no further comments are needed.

5 - NEAR FIELD EFFECTS

So far we have presented the results of a computation in which the hypothetical detector is assumed to be placed far from the undulator. Referring to fig. 1 this assumption amounts to require that the unit vector $\underline{n}$ defining the direction from which the emitted radiation is observed i.e.

$$\underline{n} = \frac{\underline{S} - \underline{r}(t)}{|\underline{S} - \underline{r}(t)|} \qquad (3)$$

is time independent since $|\underline{S}| \gg |\underline{r}(t)|$.

If the above condition is not satisfied one runs into near field difficulties. The inclusion of the unit vector time dependence in the numerical code is quite straightforward (see ref.[6]) and the results are shown in fig. 8 where the brightness of a linear undulator at $\gamma\vartheta \simeq 0.5$ is shown for different distances of the detector from the undulator. In this case at a distance equal to 8 undulator lengths the spectrum takes the far field configuration. The shape distorsion due to the near field effect is remarkable as well as the peak reduction.

We must stress that when the inhomogeneous broadening effects are not included no near field effect can be detected on axis. The situation changes with inclusion of the emittances, as shown in figs. 9.a,b, which show the distance dependence of the on axis spectrum for the third harmonic of a linear undulator. A practical formula to understand when near field effects may be important, is the following

$$\frac{S}{L} < 5\pi \, \mu_{x,y} \qquad (4)$$

where S measures the distance of the detector from the undulator entrance and L is the undulator length.

The above formula is qualitative and has been derived empirically from the numerical data; a different semi-analytical justification has been also given in ref.[5].

6 - SPECTRA FROM A MEASURED UNDULATOR

In the previous sections we have considered electron trajectories calculated from a given analytical magnetic field distribution. In a real experiment however the field distribution is not analytically known but measured. The electron trajectories must be therefore inferred from the experimental field map. This is the case shown in fig. 10.a where the x and y components of the electron motion are shown with the relevant spectrum. The undulator parameters are those relevant to the ENEA Frascati permanent magnet undulator[8] and are specified in tab. 2.

The poor quality of the spectrum shape displayed in fig. 10.a is due to the fact that the undulator field is not suitably compensed. Fig. 10.b are otherwise relevant to the case of compensed undulator and the spectrum shape is very much close to the ideal case.

Table 2. Undulator magnet characteristics

Period λ_u [cm]	5
length L [m]	2.25
Working gap [mm]	13-24
Homogeneous bandwidth $\lambda_u/2L$	0.011
Undulator parameter K	1-2
Remanent field [kG]	9.5
Number of blocks per period	4
Block dimensions [cm^3]	1.25x1.25x5
Block disposition	Halbach

7 - CONCLUSIONS

We have presented a synthetic description of a numerical code which has displayed its flexibility in treating a large number of possible parameters configurations.

The developed code may be usefully utilized to understand the result of the experiment once the undulator and the electron beam characteristics are known. Conversely it can be an effective diagnostic tool to infer the beam qualities from the obtained experimental spectra. Furthermore according to what we have discussed it may be usefully applied to understand the undulator characteristics.

Acknowledgements

It is a pleasure to thank A. Renieri for kindly providing the necessary experimental informations on the ENEA Frascati undulator.

BIBLIOGRAPHY

[1] H. Winick and S. Doniach: "Synchrotron radiation research", Plenum Press New York (1980).

[2] G. Dattoli and A. Renieri: "Experimental and theoretical aspects of the free-electron laser", Laser Handbook vol. IV, M. L. Stitch and M.S. Bass eds. North-Holland, Amsterdam (1985).

[3] D.F. Alferov, Yu.A. Bashmakov and E.G. Bessonov: Proceedings of the P.N. Lebedev Physics Institute, 80, 97 (1976).
W.B. Colson, G. Dattoli and F. Ciocci: Phys. Rev., A31, 828 (1985)

[4] R. Barbini, G. Vignola: "The L.E.L.A. undulator as a source of synchrotron radiation", Adone, Internal Memo. G-32 (1979).

[5] M. Castellano, N. Cavallo, F. Cevenini, M.R. Masullo, P. Patteri, R. Rinzivillo, S. Solimeno and A. Cutolo: Nuovo Cimento B, 81, 67 (1984).

[6] R. Barbini, F. Ciocci, G. Dattoli and L. Giannessi: to be published in Rivista del Nuovo Cimento.

[7] J.D. Jackson: "Classical Electrodynamics", J. Wiley & Sons (1975).

[8] F. Ciocci, E. Fiorentino, A. Renieri and E. Sabia: SPIE 582 169 (1985).

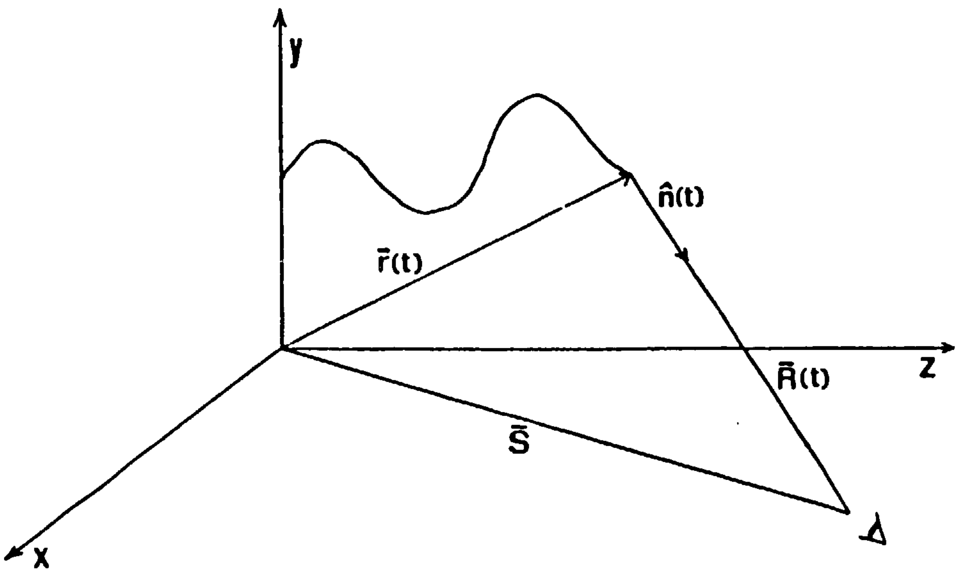

Fig. 1 Electron trajectory in the chosen reference frame.

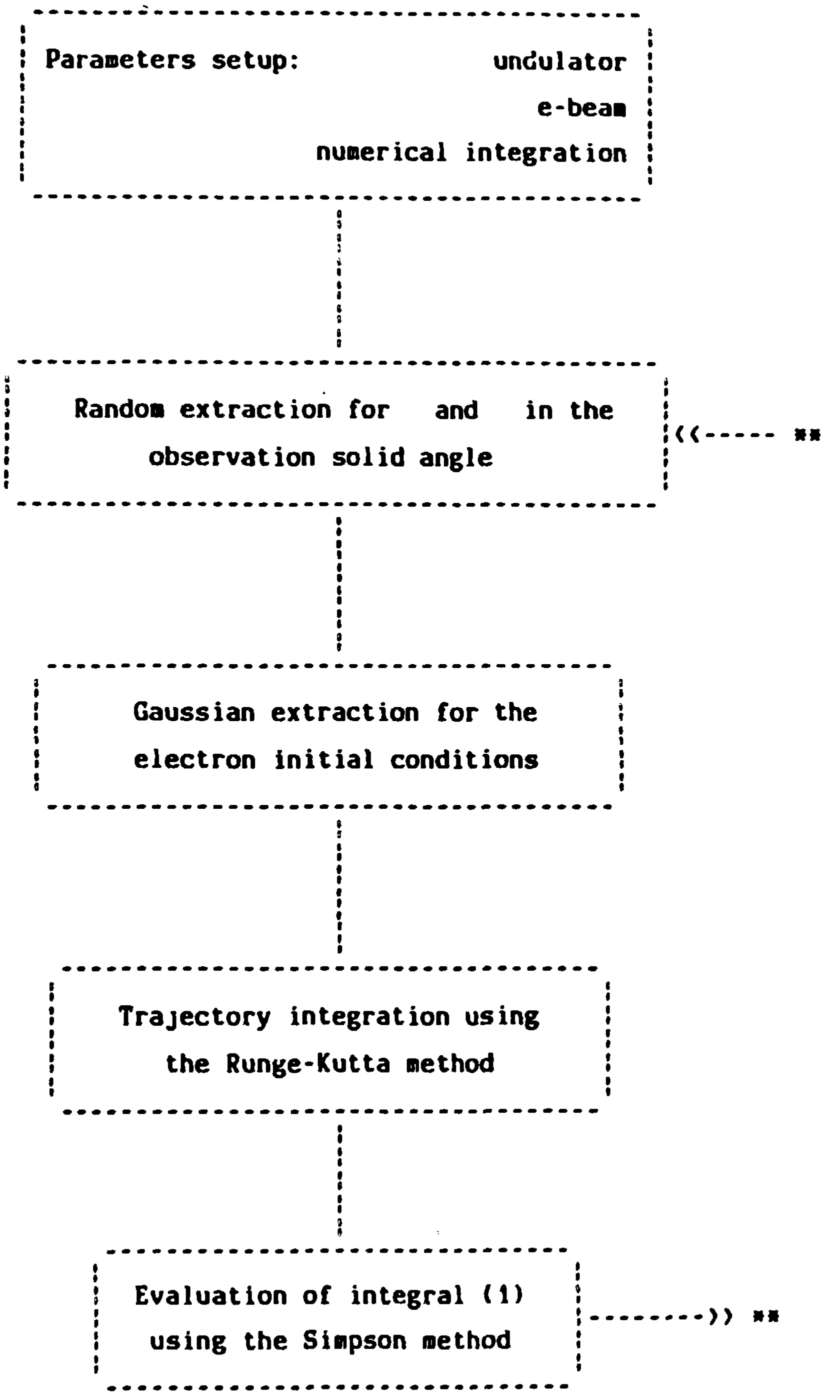

Fig. 2 Block scheme of the S-Luce code.

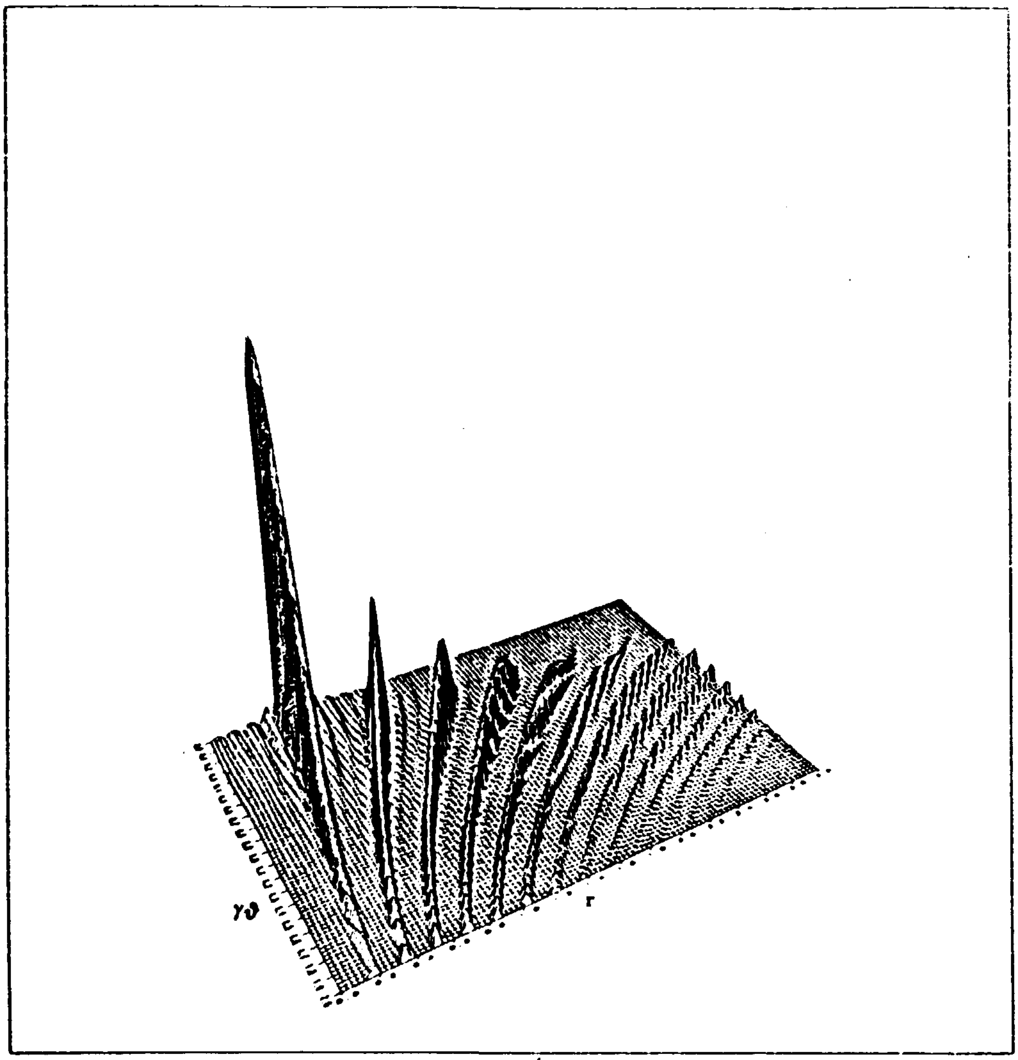

Fig. 3.a Spectral brightness 3-dimensional plot of the radiation emitted in helical undulator (5 periods, K=1.) vs. $r = \omega/2\gamma^2\omega_o$ and $\gamma\vartheta$.

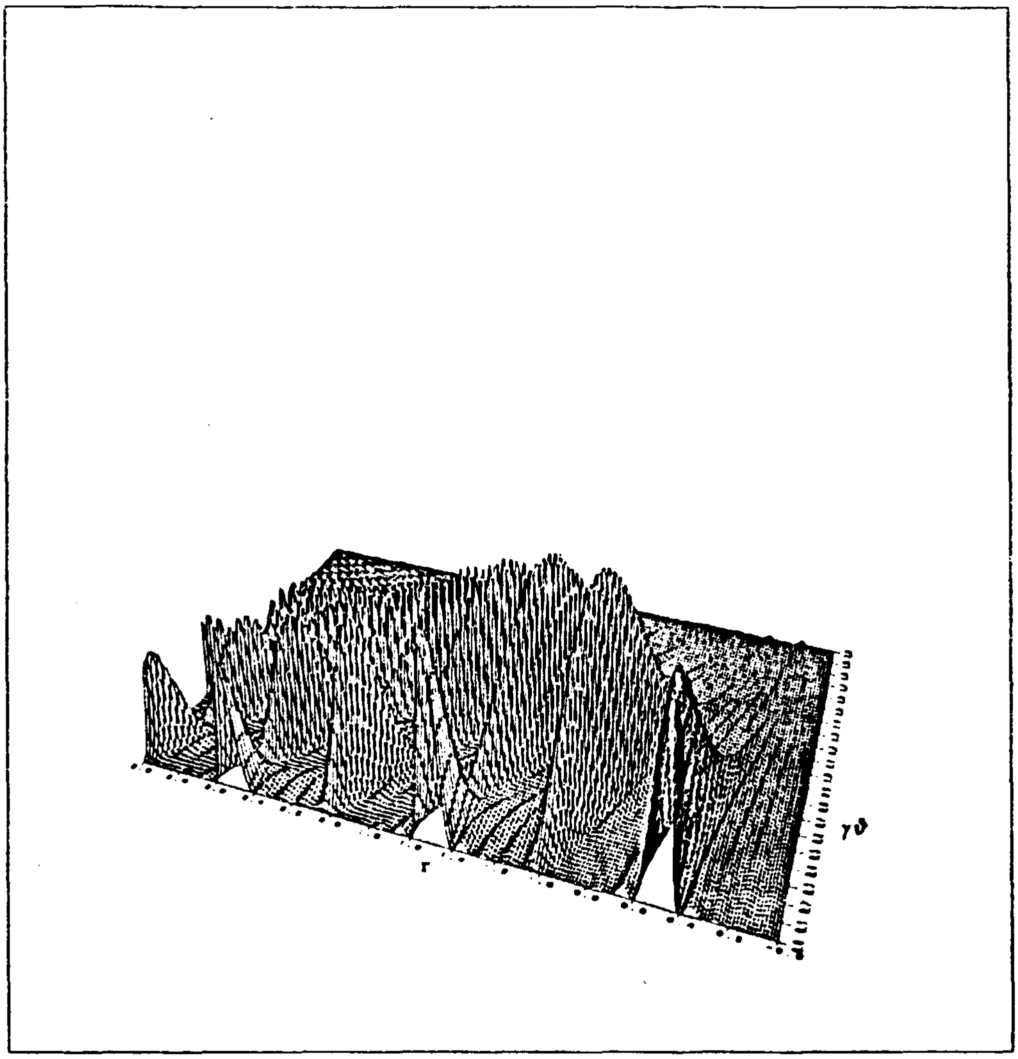

Fig. 3.b Spectral brightness 3-dimensional plot of the radiation emitted in linear undulator (5 periods, K=1.) vs. r and $\gamma\vartheta$ (φ=0).

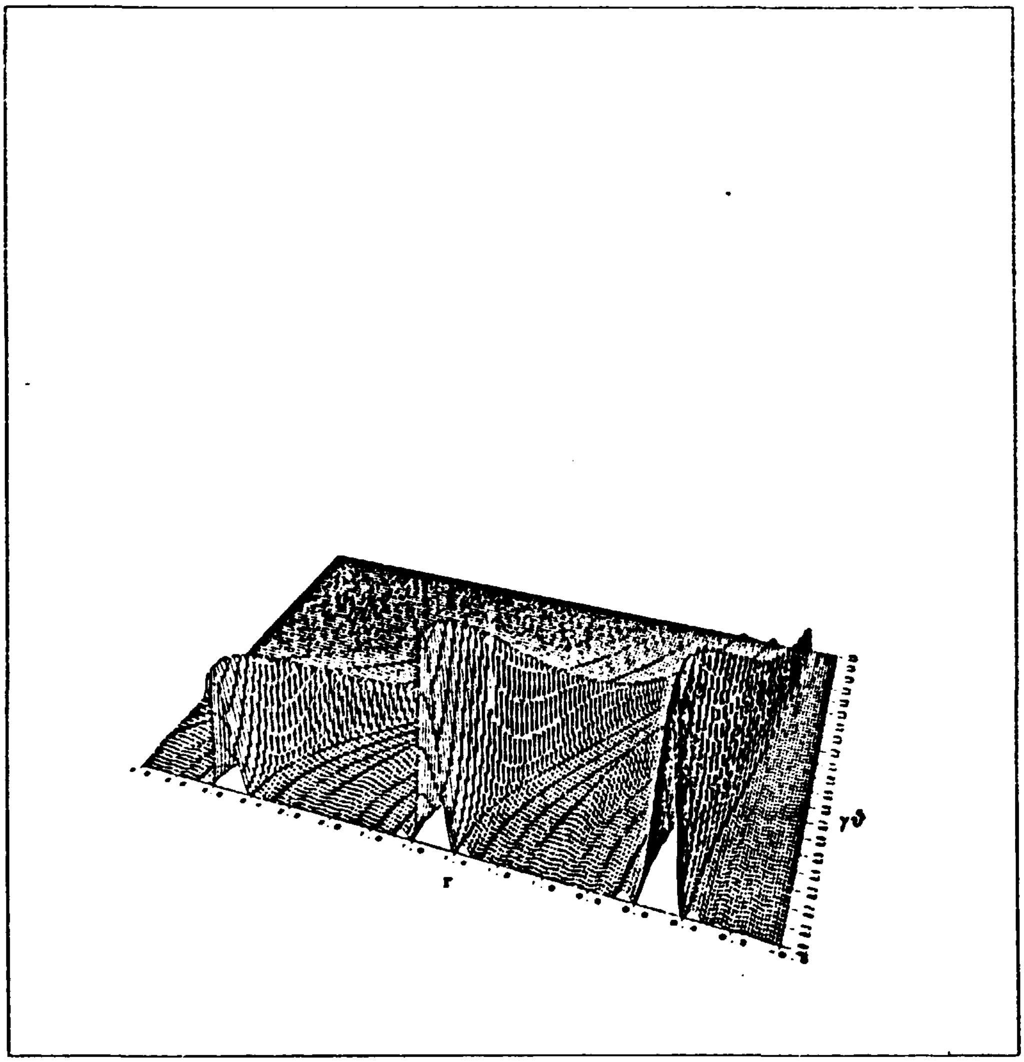

Fig. 3.c Spectral brightness 3-dimensional plot of the radiation emitted in linear undulator (5 periods, K=1.) vs. r and $\gamma\vartheta$ ($\varphi = \pi/2$).

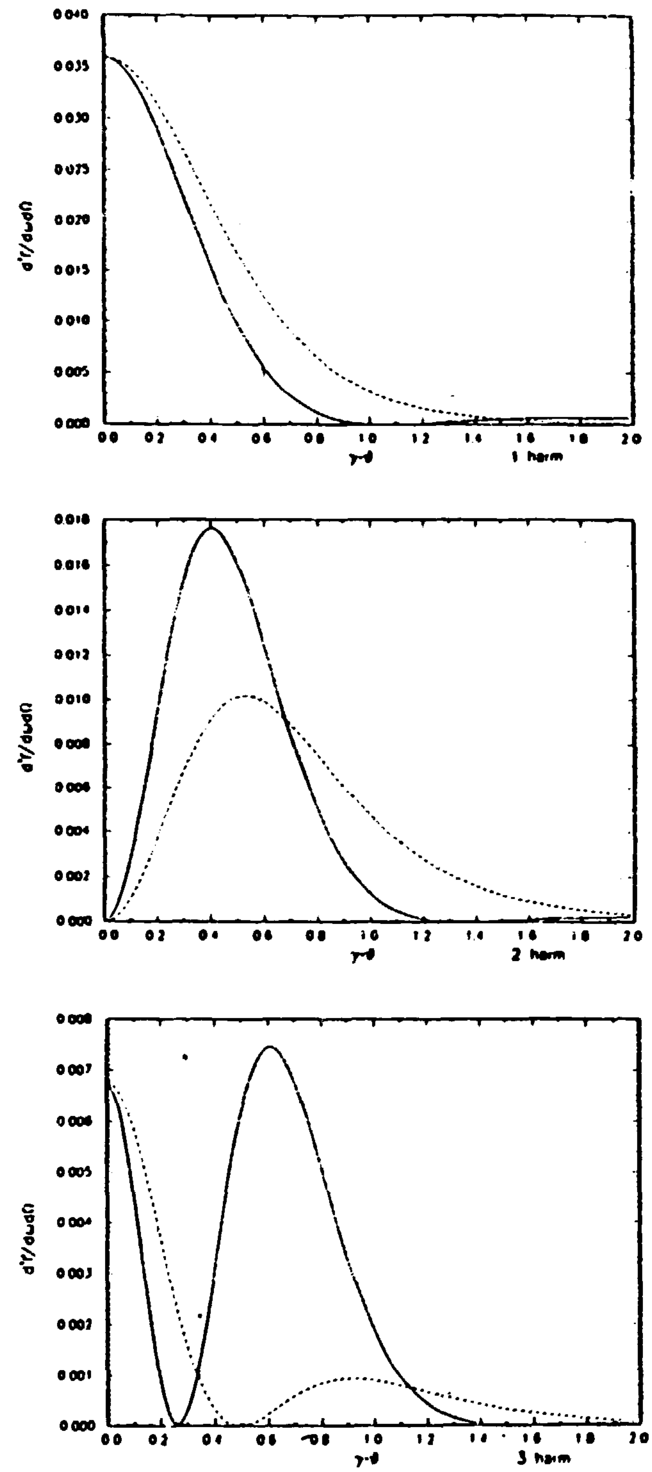

Fig. 4 Peak intensity of the first three harmonics from a linear undulator (20 periods, K=0.5) vs. $\gamma\vartheta$ (φ=0).

The following dimensionless quantity is plotted: $\frac{d^2 I'}{d\omega\, d\Omega} = \frac{1}{I_0} \frac{d^2 I}{d\omega\, d\Omega}$

where $I_0 = 8(e\gamma^2 N)/c$.

Analytical theory - dotted line, Numerical result - solid line

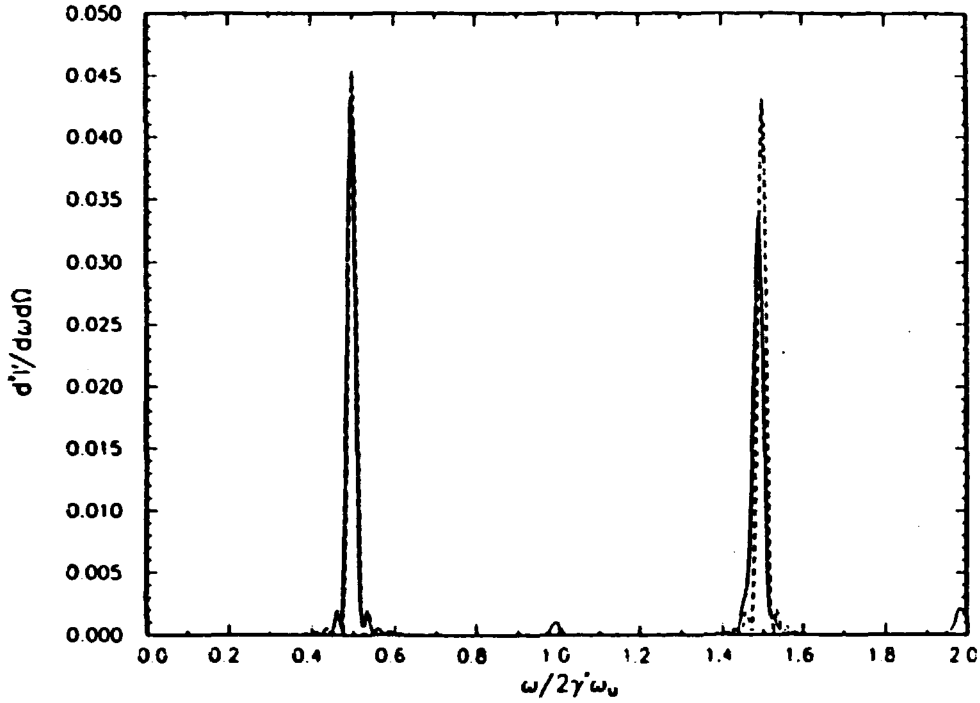

Fig. 5 Spectral brightness vs. r. Inhomogeneously broadened regime.
Linear undulator parameters :

λ_u = 5 cm K=1. 20 periods

Beam parameters :

σ_ϵ =0.001 (μ_ϵ =0.08)

E_x =6π mm mrad (μ_x =0.08)

E_y =2π mm mrad (μ_y =0.20)

γ_0 =39.14 (20 Mev)

Observer/undulator distance S=100 m $\gamma\vartheta$=0.0 φ=0.0

(dotted line / homogeneous regime).

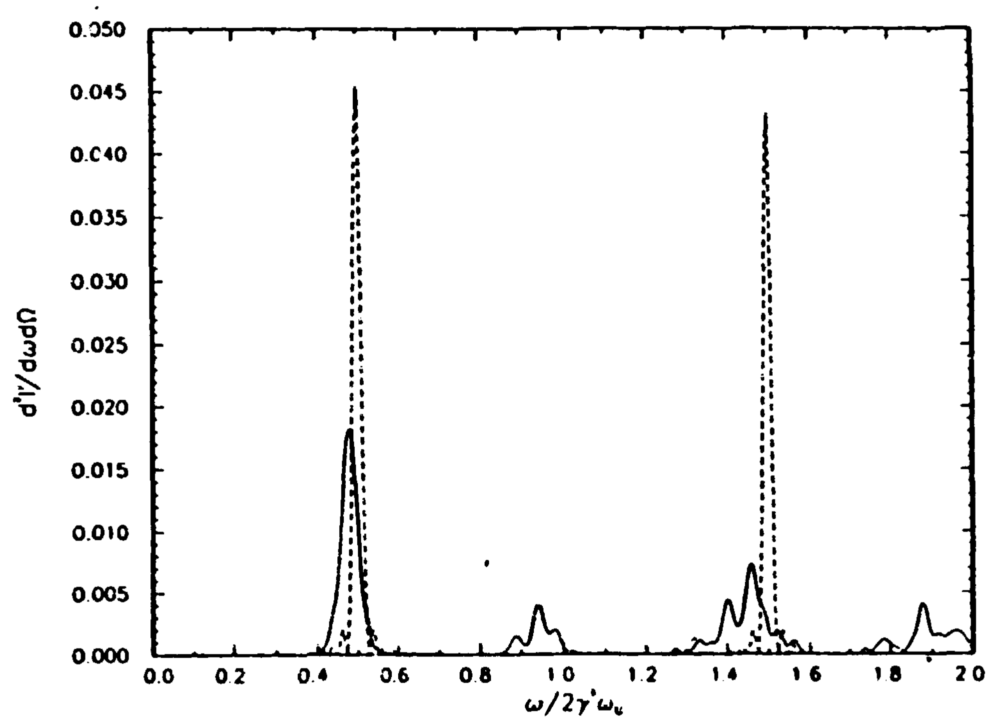

Fig. 6 Spectral brightness vs. r. Inhomogeneously broadened regime.

Linear undulator parameters :

λ_u = 5 cm K=1. 20 periods

Beam parameters :

σ_ε =0.0125 (μ_ε =1)

E_x =76 mm mrad (μ_x =1)

E_y =10 mm mrad (μ_y =1)

γ_0 =39.14 (20 Mev)

Observer/undulator distance S=100 m $\gamma\vartheta$ =0.0 φ=0.0

(dotted line / homogeneous regime).

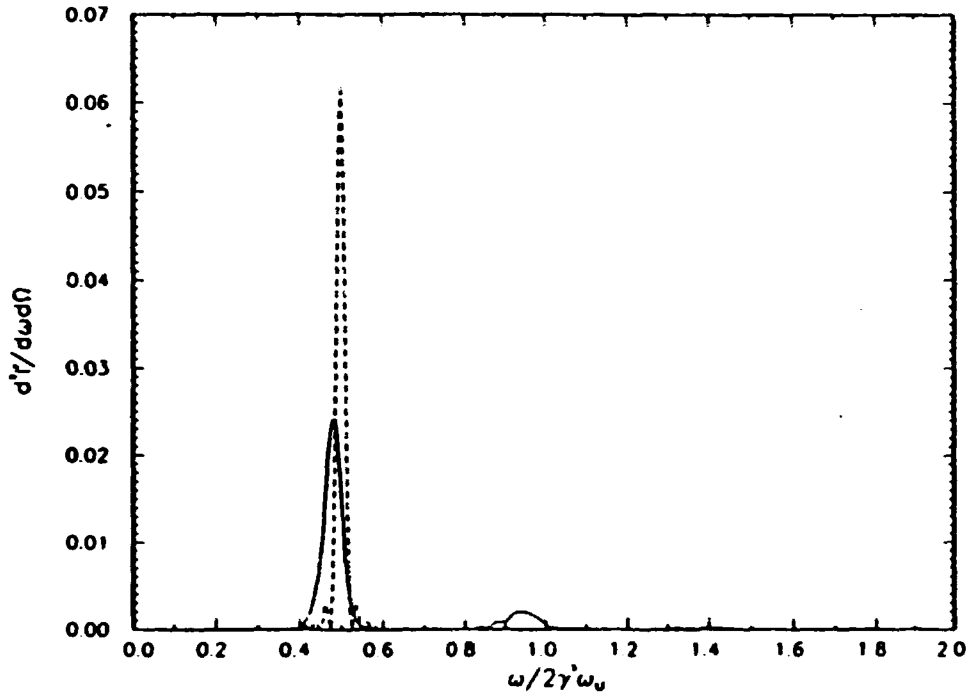

Fig. 7 Spectral brightness vs. r. Inhomogeneously broadened regime.
Helical undulator parameters :

λ_u = 5 cm K=1. 20 periods

Beam parameters :

	σ_e =0.0125	(μ_e =1)
	E_x =14 mm mrad	(μ_x =1)
	E_y =14 mm mrad	(μ_y =1)
	γ_0 =39.14	(20 Mev)
Observer/undulator distance	S=100 m $\gamma\vartheta$ =0.0	φ =0.0

(dotted line / homogeneous regime).

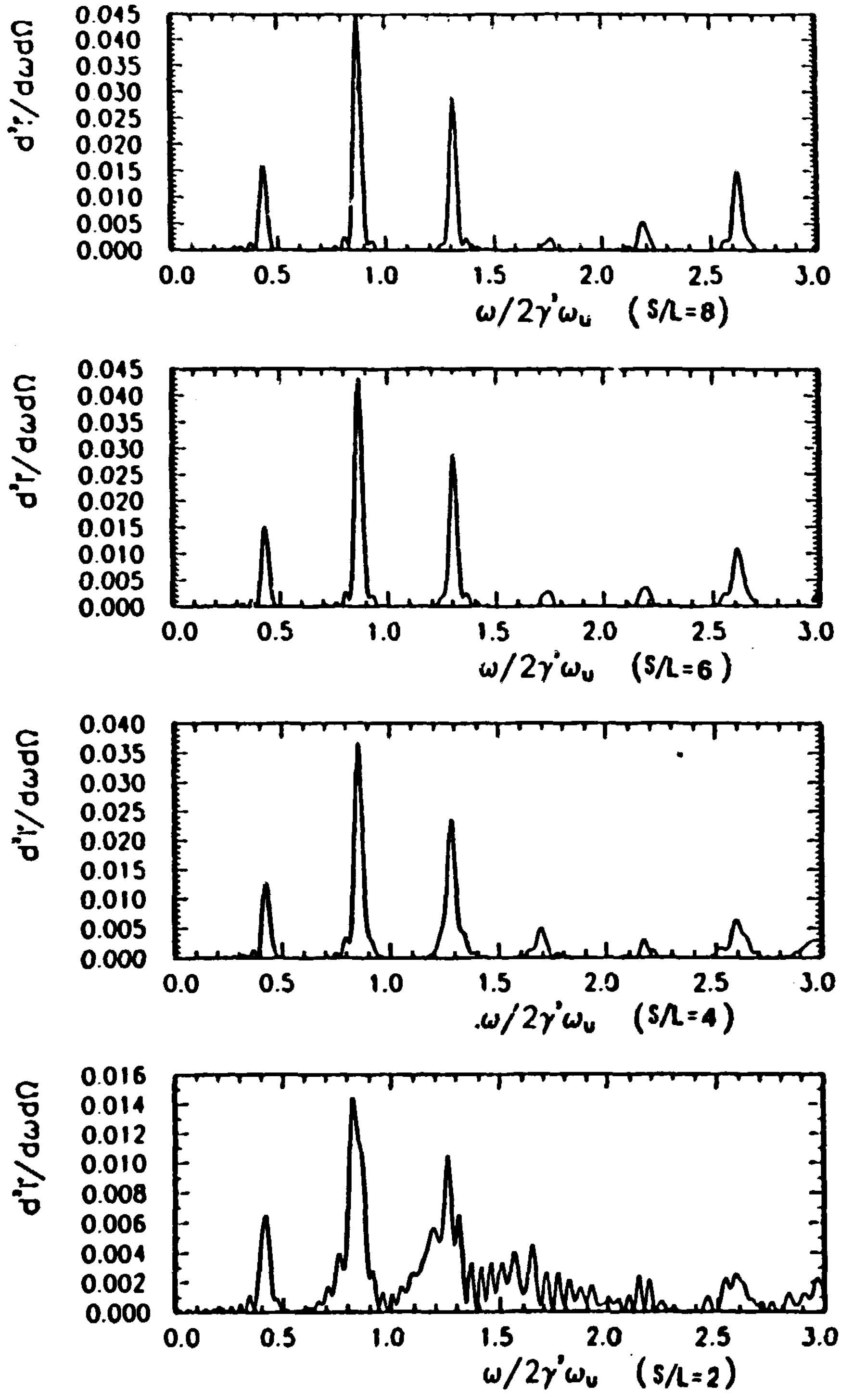

Fig. 8 Frequency plot of the linear undulator spectral brightness at different observer/undulator distances ($\gamma\vartheta=0.5$).

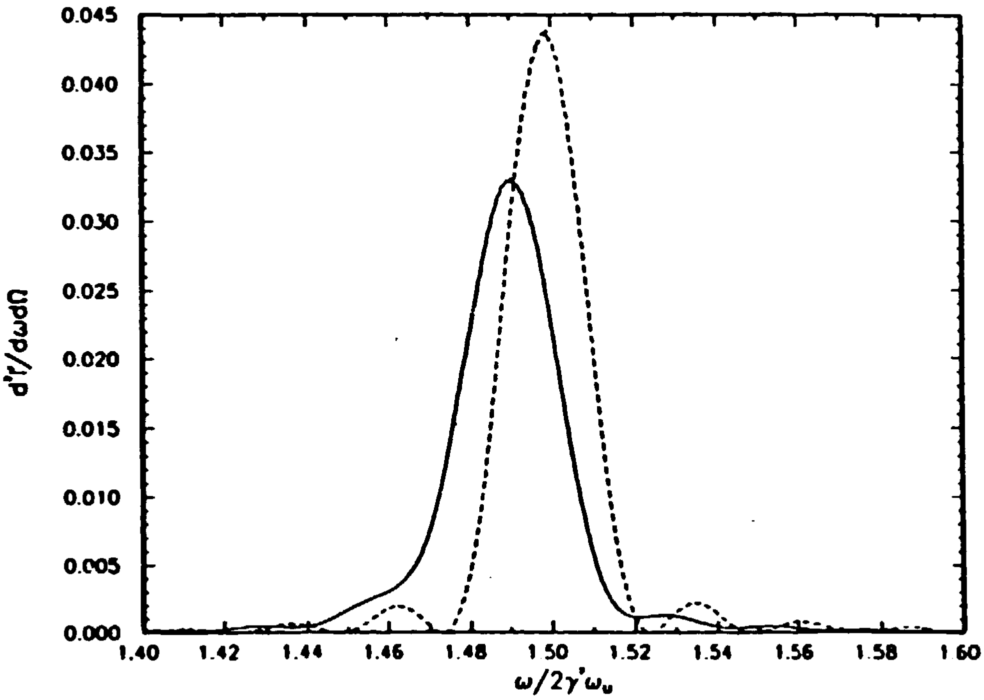

Fig. 9.a Spectral brightness vs. r. Inhomogeneously broadened regime.
Linear undulator parameters :

λ_u = 5 cm K=1. 20 periods

Beam parameters :

σ_ϵ =0.001 (μ_ϵ =0.08)

E_x =6 mm mrad (μ_x =0.08)

E_y =2 mm mrad (μ_y =0.20)

γ_0 =39.14 (20 Mev)

Observer/undulator distance S=100 m $\gamma\vartheta$=0.0 φ=0.0

(dotted line / homogeneous regime).

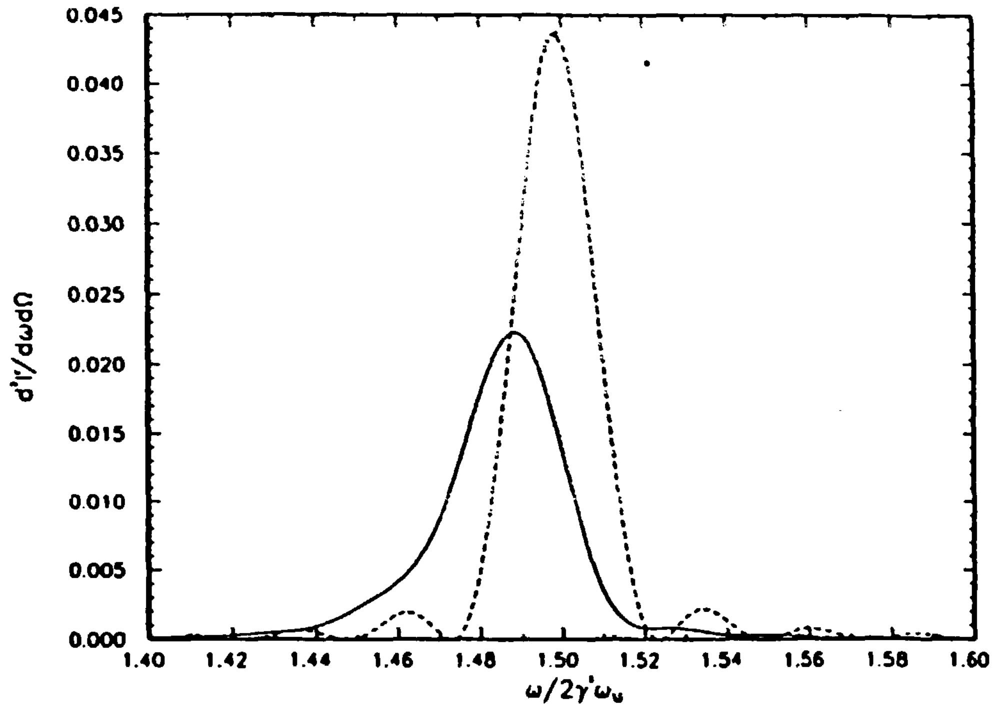

Fig. 9.b Spectral brightness vs. r. Inhomogeneously broadened regime.
Linear undulator parameters :

λ_u = 5 cm K=1. 20 periods

Beam parameters :

σ_ϵ =0.001 (μ_ϵ =0.08)

E_x =6 mm mrad (μ_x =0.08)

E_y =2 mm mrad (μ_y =0.20)

γ_0 =39.14 (20 Mev)

Observer/undulator distance S=1.5 m $\gamma\vartheta$=0.0 φ=0.0

(dotted line / homogeneous regime).

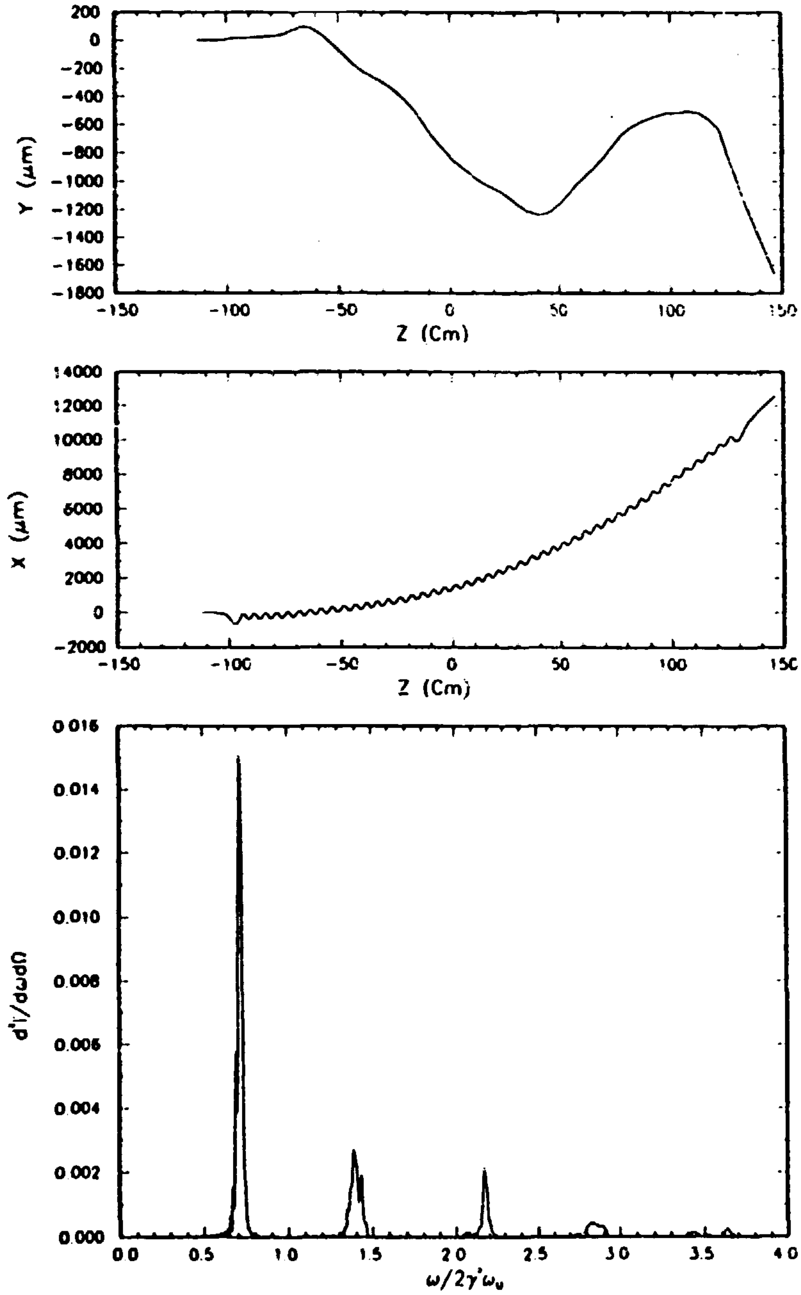

Fig. 10.a Electron trajectory in measured undulator field (uncompensed) and the relevant on axis spectrum.

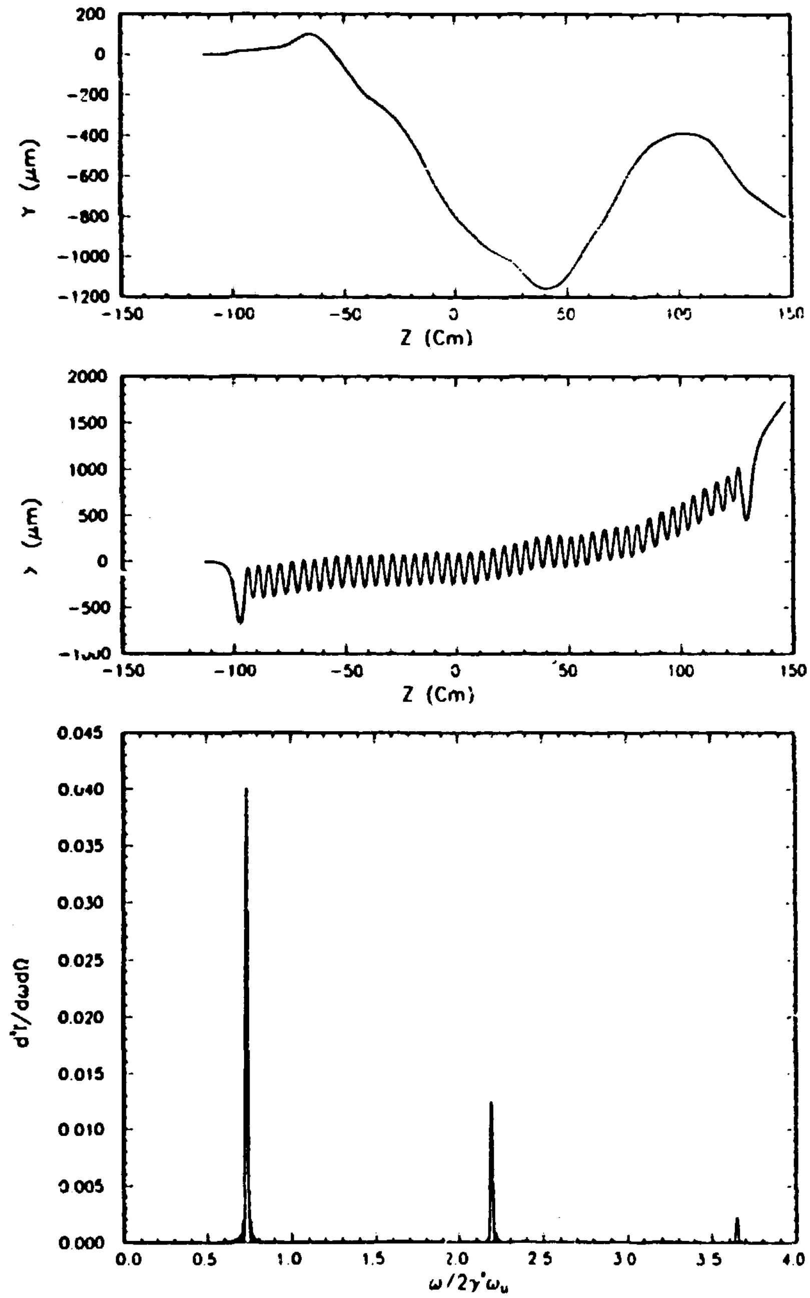

Fig. 10.b Electron trajectory in measured undulator field (compensed) and the relevant on axis spectrum.

Edito dall'ENEA, Direzione Centrale Relazioni
Viale Regina Margherita, 125 - Roma
Finito di stampare nel mese di novembre 1987
Fotoripr. e Stampa «Arti Grafiche S. Marcello»
Viale Regina Margherita, 176 - 00198 Roma